



Encapsulation of thyme and cinnamon essential oils in porous corn starch: particle size, microstructure, and antimicrobial properties

Jasim Ahmed¹ · Linu Thomas¹ · Sarah Al-Jassar¹ · Harsha Jacob¹ · Mehraj Mulla¹ · Noor Al-Ruwaih¹

Received: 11 May 2023 / Accepted: 7 July 2023 / Published online: 15 July 2023

© The Author(s), under exclusive licence to Springer Science+Business Media, LLC, part of Springer Nature 2023

Abstract

Encapsulation of essential oils into a suitable, inexpensive wall material is the best strategy for their further use in food and pharmaceutical applications. In this work, porous corn starch was produced by enzymatic hydrolysis and used as a wall material for the entrapment of thyme and cinnamon essential oils. The properties of those encapsulated microcapsules were measured using various analytical techniques. The micrographs of porous corn starch demonstrated that enzymatic hydrolysis resulted in a significant number of pores. The mean volumetric particle size ($D_{v,50}$) of porous starches did not differ significantly (16.3- μm) from the native starch (16.6- μm). The encapsulated microcapsules aggregated, and the $D_{v,50}$ increased significantly higher than the porous corn starch. The melting temperature and process enthalpy of porous starch increased when compared to native starch. The characteristic thermograms of essential oils did not appear in the microcapsules, confirming the formation of a strong complex. The essential oil/porous starch microcapsules showed antimicrobial activity against *Listeria monocytogenes* and *Salmonella enterica* sv. Typhimurium. The obtained results provide information on the thermal stability and antimicrobial properties of essential oil-incorporated microcapsules so that they could be formulated into active packaging applications.

Keywords Porous corn starch · Enzymatic hydrolysis · Particle size distribution · Essential oil · Microstructure

Introduction

Green consumerism motivates industries to adopt nature-derived ingredients in food and drug formulations, food packaging, and other applications [1]. Plant-derived essential oils (EOs) are the most desired active ingredients in the food, pharmaceutical, and cosmetic industries, and are currently being extensively explored. EOs are secondary metabolites from plant sources and aromatic liquids extracted from various parts of plants and rich in volatile compounds (e.g., aldehydes, ketones, terpenes, alcohols, esters, and phenols) that possess excellent antibacterial, antiviral, antifungal, and antioxidant abilities [2–8]. Among volatile essential oils, thyme essential oil (TEO) and cinnamon essential oil (CEO) have wide acceptability in the

food and pharmaceutical industries for their broad antimicrobial activities against many food-borne pathogens (e.g., *Escherichia coli*, *Listeria monocytogenes*, *Salmonella* sp., *Staphylococcus aureus*), and spoilage bacteria [2, 9, 10]. Additionally, both EOs are listed as “Generally Recognized as Safe” (GRAS) by the U.S. Food and Drug Administration. Cinnamaldehyde is the key component of cinnamon oil, whereas thymol, carvacrol, and paracymene are major constituents responsible for imparting most of the desired properties of thyme essential oil [11]. Therefore, it is anticipated that both of these EOs could be considered potential candidates in food preservation, drug delivery, and active packaging.

The bioactive compounds in EOs have poor solubility and bioavailability, high volatility, heat, pH, and light sensitivity [12], which challenges their applications in the industry. To overcome those limitations, the entrapment of EO in a suitable wall material (commonly referred to as microencapsulation) can be a prospective approach to reduce their degradation, improve their bioavailability, and maintain a controlled release of entrapped volatiles at a selected target [13, 14]. The encapsulation technique has

✉ Jasim Ahmed
jahmed2k@yahoo.com; jaahmed@kisar.edu.kw

¹ Food & Nutrition Program, Environment and Life Sciences Research Center, Kuwait Institute for Scientific Research, P.O. Box 24885, Safat 13109, Kuwait

generated a higher demand for products containing EOs in many industries, including food, pharmaceuticals, textiles, detergents, perfumery, and personal care [15]. A range of wall materials, including cyclodextrins, chitosan, sodium alginate, modified starch, and maltodextrin, have been used for the encapsulation and controlled release of EOs. Earlier, a comparison was made between two cyclodextrins (β - and γ -cyclodextrin) for the encapsulation of EOs, and it was found that γ -cyclodextrin showed a superior wall material compared to its counterpart [1, 16]. A range of wall materials and their potential applications have been elaborately discussed in a recent review [17].

In the encapsulation process, the commercial viability of wall materials plays an important role in their selection. Among the wall materials used, starch is one of the most promising candidates because of its inexpensiveness, non-toxicity, ecological sustainability, and compatibility with food ingredients. Starch as such (e.g., native) cannot serve as the wall material because it has poor properties to form emulsions, which is a prerequisite for the encapsulation systems of EOs [18]. The development of micro-sized pores in the starch surface can absorb more bioactive compounds because of its large surface area and produce stable emulsions. A combination of enzymes (α -amylase and glucoamylase) and [α -amylase (AM) or amyloglucosidase (AMG)] can be an effective technique to obtain porous starch [19, 20]. The release of active compounds from the starch inclusion complex, however, is not easy, and therefore, it needs to be addressed adequately. The addition of hydrocolloids (e.g., Arabic, xanthan gum) to EO to form an emulsion could improve the apparent viscosity, resulting in the formation of a thin layer around the porous starch surface. Wu et al. [21] used porous rice starch (PS) and Xanthan gum (XG) to incorporate curcumin at different ratios, and they produced excellent curcumin-loaded microcapsules.

Considering all those facts discussed above, the current work is focused on developing porous corn starch (PCS) using enzymatic hydrolysis and its capability to form inclusion complexes of thyme essential oil (TEO) and cinnamon essential oil (CEO) in the PCS matrix. The antimicrobial, thermal, and particle morphologies of the developed microcapsules were further evaluated using various analytical tools.

Materials and methods

Materials

Pure corn starch with an amylose content of about 24% (Argo, ACH Food, Cordova, TN) was purchased locally. Highly purified α -amylase (AM) (3,000 U/mL) from *Bacillus* sp.

and amyloglucosidase (AMG) (3,260 U/mL) from *Aspergillus niger* were obtained from Megazyme International (Ireland). Cinnamon essential oil (CEO; Ceylon-type; yellow to dark brown in color; refractive index: 1.53–1.54 and specific gravity: 1.03–1.05 g/mL at 20 °C) and thyme essential oil (TEO; France-origin; colorless to pale yellow; refractive index: 1.50–1.51 and specific gravity: 0.905 to 0.935 g/mL at 20 °C) were procured from Sigma-Aldrich (St. Louis, MO, USA). Fisher Scientific (Loughborough, LE, UK) supplied ethyl alcohol.

Bacterial strains and media

The gram-negative *Salmonella enterica* sv. Typhimurium (ATCC 14,028) strain and the gram-positive *Listeria monocytogenes* (ATCC 7644) strain Culti-loops® were obtained from Thermo Fisher Diagnostics B.V. (The Netherlands) and Remel Europe Ltd. (Dartford, Kent, UK), respectively. Trypticasein Soy Agar (TSA) was procured from Conda Laboratories (Torrej on de Ardoz, MD, Spain). Tryptic soya broth (TSB) and buffered peptone water (BPW) were obtained from Oxoid Limited (Basingstoke, Hampshire, UK). All the other chemicals used in this study were of analytical reagent grade.

Preparation of porous corn starch by enzymatic hydrolysis

To produce a porous surface of corn starch, the method described by Wu et al. (2020) was adopted with some modifications. Briefly, corn starch (10 g, dry basis) was dispersed in 40 mL of 0.2 M citric acid–sodium citrate buffer at pH 4.0 by sonication (Branson Digital SFX-250 Sonifier; Marshall Scientific; Hampton, NH) at 25 °C for 30 min. For enzymatic hydrolysis, a mixture of the enzymes [AM (200 μ L of 1U/mL) and AMG (4 mL of 3260 U/mL)] was transferred to the starch dispersions. Samples were shaken in a water bath at 150 rpm for 16 h at 40 °C. The reaction was terminated by the addition of 2 mL of NaOH solution (0.4%). Samples were centrifuged at 3000 rpm for 15 min; the sediment was re-suspended in deionized water, and centrifuged three times more following similar conditions. The final sediment was dried in a drying oven at 50 °C until a constant weight was achieved. Finally, the porous starch (PS) was ground to powder, and sieved through a 200-mesh sieve. Three batches of samples were prepared.

Encapsulation of essential oil and xanthan gum emulsion in starch dispersion

The microencapsulation of EO (CEO and TEO) with porous starch/xanthan gum was performed according to Trindade

and Grosso (2000) with some modifications. 1 g of EO was added to an aqueous solution of 0.25% aqueous xanthan gum (XG) solution (2 mL) intermittently. The mixture was prepared by continuously stirring at room temperature for 16 h. Then 2 g of porous corn starch was slowly added to the mixture of oil and gum. The mixture was homogenized and stirred in a covered beaker for 20 h at room temperature. The samples were dried at 50 °C in a hot-air oven and stored at 4 °C for further analysis.

Characterization

Moisture content and bulk density

The moisture content of samples was determined by the oven drying method (105 °C/4 h). The bulk density (ρ_b) of the powdered samples was calculated when the volume was measured after transferring 1 gram of powder into a graduated 10 ml cylinder without any consolidation [1, 16]. All experiments were conducted in triplicate.

Color measurement

The color of the powders was measured using a colorimeter (LabScan XE, Hunter Associates Laboratory, Reston, VA) [5]. The instrument was calibrated with standard white and black tiles. Three primary color parameters, namely *L* (lightness), *a* (redness and greenness), and *b* (yellowness and blueness), were recorded directly from the instrumental software.

Water holding capacity and oil holding capacity

The water holding capacity (WHC) and oil holding capacity (OHC) of samples were measured following the centrifugal techniques at 25 °C [22].

Morphology

The microstructures and particle dimensions of the dried powders were scanned using a scanning electron microscope (SEM) (JEOL, JCM-6000 Plus, Tokyo, Japan) with an acceleration potential voltage of 15 keV following our earlier work [1, 16]. Powdered samples were mounted on stubs, and a thin layer of chromium was used for coating. Each sample was photographed at magnifications of 450× and 1500×. Measurements were made in duplicate.

FT-IR analysis

The ATR-FTIR analysis was conducted with a Nicolet iS5 FTIR Spectrometer (Thermo Scientific, Madison, WI,

USA) to assess the incorporation of the EO into the matrices of the porous starch matrix [1, 16]. A total of 32 scans were recorded in the range of 4000 to 550 cm^{-1} with a resolution of 4 cm^{-1} .

Thermal analysis

Thermal analysis of EO, native, and porous corn starch samples was performed on a Q2000 DSC (TA Instruments, New Castle, DE) following our earlier method [1]. The instrument was calibrated with indium and sapphire for temperature and heat capacity calibration. The samples in aluminum pans (8 mg) were thermally scanned from 0 to 300 °C at a rate of 10 °C/min in heating/cooling cycles in a nitrogen atmosphere (flow rate, 50 mL/min). An empty pan was used as a reference. Instrument software (version 4.5 A, TA Instruments, New Castle, DE, USA) was used to perform thermal analysis.

Encapsulation efficiency

The encapsulation efficiency (EE) of powdered encapsulates was assessed following the method described by Huang et al. [23]. A full-wavelength scan of the diluted EO was conducted to determine its peak absorption wavelength. Selected concentrations of EO (0.04–0.20 mg.L⁻¹) were made to obtain a standard curve. In brief, 0.05 g powdered encapsulate was dispersed in 5 mL of ethyl alcohol and sonicated at 40 °C for 5 min. Then the solution was transferred to a 50 mL volumetric flask and the volume was adjusted with ethanol. Thereafter, 10 mL of the solution was centrifuged at 8000 ×g for 10 min at 4 °C. The absorbance of the supernatant was measured at 275 nm using a UV–visible spectrophotometer (Shimadzu UV-1800, Kyoto, Japan). The encapsulation efficiency (EE) was calculated following Eq. (1).

$$\% \text{Encapsulation efficiency} = \left[\frac{\text{Weight of EO in microcapsules (mg)}}{\text{Initial EO weight (mg)}} \right] \times 100 \quad (1)$$

Particle size distribution

The particle size distribution (PSD) of the dried powder samples in water was conducted by a Mastersizer 3000 laser diffraction particle size analyzer (Malvern Instruments Ltd., UK) attached with a Hydro MV accessory [1, 16]. The PSDs at 10%, 50% (median diameter), and 90% are presented as D_{v10} , D_{v50} , and D_{v90} , respectively. The polydispersity of the particles is calculated in terms of ‘span’.

Assessment of antimicrobial activity of essential oils encapsulated powders

Two test strains of *Listeria monocytogenes* (Gram-positive) and *Salmonella enterica* sv Typhimurium (Gram-negative) were selected as model bacteria to assess the antibacterial activity of free EO (CEO and TEO) and EO-loaded microcapsules using the macro-broth dilution method. Details are available elsewhere [16, 23]. Both pathogens were revived in TSB at 37 °C for 24 h in an incubator so that the concentration of strains was maintained at 10^8 colony forming units (CFU mL⁻¹) in buffered peptone water. The stock suspensions of PCS/EO made in ethanol and water (1:1) were diluted in sterile TSB and inoculated with an adequate volume of 10^8 CFU/mL of bacterial cell cultures to obtain a desired concentration. The concentrations were varied from 1500 to 5000 µg/mL and 750 to 5000 µg/mL for PCS/EO/XG and EO, respectively. A TSB comprising the same concentration of bacteria was used as a control. After shaking the bacterial solution at 150 rpm at 37 °C for 24 h, 100 mL of diluted culture was spread on the TSA plate. The plates were incubated at 37 °C for 24 h before counting the colonies. Results were presented as log CFU/mL. Microbiological experiments were performed in triplicate.

The Minimum Bactericidal Concentration (MBCs) of free and encapsulated EO was taken as the lowest concentration where no visible growth was detected in the plates after the incubation period of 24 h.

Statistical analysis

JMP Pro 17 Statistical Software (SAS Institute Inc., Cary, NC, USA) was employed for statistical analysis of the experimental data. The data are presented as the means ± standard

deviations of at least three independent measurements for each sample and were subjected to analysis of variance (ANOVA) and Tukey's test for comparison between mean values at a 95% confidence level ($p < 0.05$).

Results and discussion

Moisture content and bulk density

The moisture content of the native CS was 1.35% on a dry basis, which decreased significantly to 0.07% and 0.75% upon enzyme treatment and gelatinization, respectively, followed by drying (Table 1). The moisture contents were found to be higher in the IC samples when compared to the PCS, in particular, PCS/TEO, and the values differed between samples prepared by the two different techniques. Differences in the moisture contents in two methods of EO inclusion could be associated with the rate of drying, encapsulation efficiency, and hygroscopicity of the materials [16].

Bulk density measures the particles occupying a defined volume and remains one of the important parameters for transporting and packaging powdered materials. As can be seen in Table 1, the bulk density of the CS was 550 kg/m³, which was reduced significantly ($p < 0.05$) in the range of 510 to 520 kg/m³ as expected for the PCS samples, indicating the light weight of the PCS. Upon incorporation of EO into the PCS matrix, the bulk density dropped significantly, and those values ranged between 420 and 500 kg/m³. The IC containing TEO in XG had the lowest value of bulk density because of the thin film formation at the surface of the PCS and occupied more volume in a specified space.

Color Parameters

The color values of the native CS were: $L^* = 95.44 \pm 0.78$, $a^* = -0.55 \pm 0.09$, and $b^* = 4.13 \pm 0.48$ (Table 1). The lightness decreased with the treatment, and those values were reduced to 93.80 ± 0.11 and 90.59 ± 0.14 for enzyme and hydrothermal treatment, respectively. The greenness ($-a^*$) and yellowness ($+b^*$) of PCS decreased from -0.55 ± 0.09 to 0.32 ± 0.01 and from 4.13 ± 0.48 to 3.23 ± 0.02 with the treatments. Changes in color values are attributed to surface treatment and processing, where the pigments are affected.

The color values of the PCS altered significantly following the inclusion complex formation with EOs. The L^* value decreased to 73.78 and 81.32 for PCS/CEO and PCS/TEO using the mortar-pestle, respectively. Furthermore, those values did not differ significantly with the incorporation of XG in the PCS matrix (Table 2). Incorporation of EOs, however, incremented significantly ($p < 0.05$) both greenness (a^* : -1.49 to -0.81) and yellowness (b^* : 5.94 to

Table 1 Physical properties of native and porous corn starches

Parameters	Native corn starch	Porous corn starch
Moisture content (%)	1.35 ± 0.07^a	0.17 ± 0.01^b
Bulk density (kg.m ⁻³)	550 ± 4.11^a	520 ± 3.34^b
Water holding capacity (g/g)	2.16 ± 0.03^a	2.33 ± 0.02^a
Oil holding capacity (g/g)	1.92 ± 0.08^a	2.01 ± 0.07^a
Color value		
L^*	95.44 ± 0.78^a	93.80 ± 0.11^a
a^*	-0.55 ± 0.09^a	-0.44 ± 0.01^a
b^*	4.13 ± 0.48^a	3.23 ± 0.02^b
Particle size distribution		
D_{v10} (µm)	10.10 ± 0.59^a	9.79 ± 0.13^a
D_{v50} (µm)	16.60 ± 0.73^a	16.30 ± 0.78^a
D_{v90} (µm)	27.40 ± 1.83^a	28.40 ± 0.98^a
Span	1.04 ± 0.62^a	1.14 ± 0.62^a

All values are means ± SD, $n = 3$; values in the same row in one group with different letters are significantly different ($p < 0.05$)

Table 2 Physical properties of encapsulated porous corn starch

Parameters	PCS/CEO/XG	PCS/TEO/XG
Moisture content (%)	1.04 ± 0.02 ^a	2.66 ± 0.07 ^b
Bulk density (kg.m ⁻³)	460 ± 2.01 ^a	420 ± 2.22 ^b
Encapsulation efficiency (%)	52.23 ± 0.66 ^a	68.91 ± 0.28 ^b
Color value		
L*	73.88 ± 0.74 ^a	80.57 ± 0.52 ^b
a*	-1.16 ± 0.08 ^a	-1.03 ± 0.04 ^a
b*	14.84 ± 0.93 ^a	5.94 ± 0.56 ^b
Particle size distribution		
D _{v10} (μm)	11.3 ± 0.79 ^a	10.9 ± 0.89 ^a
D _{v50} (μm)	22.5 ± 1.11 ^a	18.8 ± 1.03 ^b
D _{v90} (μm)	81.0 ± 2.33 ^a	35.6 ± 1.58 ^b
Span	3.09 ± 0.79 ^a	1.31 ± 0.47 ^b

All values are means ± SD, n = 3; values in the same row in one group with different letters are significantly different (p < 0.05)

14.84), and those values are attributed to chlorophyll and carotenoids present in the individual EOs. The obtained color values between the two adopted techniques demonstrate that XG did not have any influence on the color of the microcapsules.

Water holding capacity and oil holding capacity

The water holding capacity (WHC) of the enzyme-assisted PCS improved to 2.33 ± 0.02 g/g when compared with the native starch (2.16 ± 0.03 g/g) at 25 °C; however, the increment was phenomenal for the sample prepared via gelatinization (5.58 ± 0.12 g/g) (Table 1). Such an abrupt increment occurred because of the special structure of porous starch attained through rigorous treatment of the native starch during the hydrothermal treatment. Xie et al. [24] found the water adsorption rate of wheat starch was higher compared to natural starch after hydrothermal treatment, which was mainly attributed to the greater number of binding sites in the amorphous regions of the samples. Therefore, the WHC of porous starch can be used as an index to characterize the pore-forming effect of starch [25]. Similarly, the oil holding capacity of native starch increased from 1.92 ± 0.08 g/g to 2.01 ± 0.07 to 2.35 ± 0.24 for porous starch created by enzymatic and hydrothermal treatment, respectively. Higher values of OHC have been reported for porous starch where enzymes were not used [26].

Encapsulation efficiency

Table 2 presents the calculated encapsulation efficiency (EE) of PCS microcapsules. The EE of microcapsules produced by the mortar and pestle method was significantly low (5.30 to 7.15%), indicating the method was not suitable for encapsulation of EO. The reason for the low EE could be poor distribution of EO onto the porous starch surface.

Concurrently, the EE of the microcapsules was significantly improved when XG was added to the EO for emulsification and the formation of an inclusion complex in the porous starch matrix. The EE was significantly higher (68.91%) for the PCS/TEO/XG microcapsule when compared with the PCS/CEO/XG (52.23%). Similar EE values have been reported in the literature [27]. The obtained results concluded that the incorporation of EO into the XG solution positively influenced the EE. All the encapsulation efficiencies were higher than 52%, which indicated that the PCS microcapsules had potential for loading EO. The difference in EE could be related to the hydrophilic/hydrophobic characteristics of individual EO and XG, followed by the surface properties of porous starch. Because of its hydrophilic nature, the XG produces a colloid solution in water and thereafter forms an emulsion with the EO. The emulsion was used to cover the surface of PCS by increasing its viscosity. Cai et al. [28] reported similar results.

Particle size distribution

The particle size distribution (PSD) of native CS and PCS demonstrated a bimodal distribution of particles; the first peak was prominent with populations ranging between 4 and 50-μm while the second peak was a marginal one exhibiting only large particles (> 750-μm) (Fig. 1). This observation is consistent with the reported values for corn starch [29]. The peak height of the first peak of the CS was reduced from 16.4-μm to 14.6-μm after the generation of porosity in the starch (Table 1). The numbers of starch particles in the volume distributions are measured in terms of D_{v10}, D_{v50}, D_{v90}, and span (S) values. The D_{v10} values of the native starch (10.1 ± 0.59-μm) were not influenced by the enzyme treatment (9.79 ± 0.13-μm) or gelatinization (11.11 ± 0.62) and the same is followed by the median values (D_{v50}) of native (16.60 ± 0.73-μm) and porous starches (16.30 ± 0.78 and 18.90 ± 0.56-μm). The D_{v90} values for the porous starch were comparable (28.4 ± 0.98-μm) to the native starch (27.4 ± 1.83-μm). Samples produced by gelatinization, however, exhibited the presence of larger particles (35.70 ± 1.97). A higher value observed for gelatinized starch could be because of the aggregation of starch particles after the hydrothermal treatment. Similar observations have been reported for atomized high-amylose starch [21] [27]. The authors reported that the aggregates formed when multiple spheres impinged upon each other in a molten or partially molten state. The span values of native (1.04 ± 0.08) and porous starch (1.14 ± 0.10) demonstrate a uniform distribution of particles.

The particle size distribution (PSD) of starches altered after the encapsulation. The microcapsules obtained by mortar and pestle did not show any significant changes in

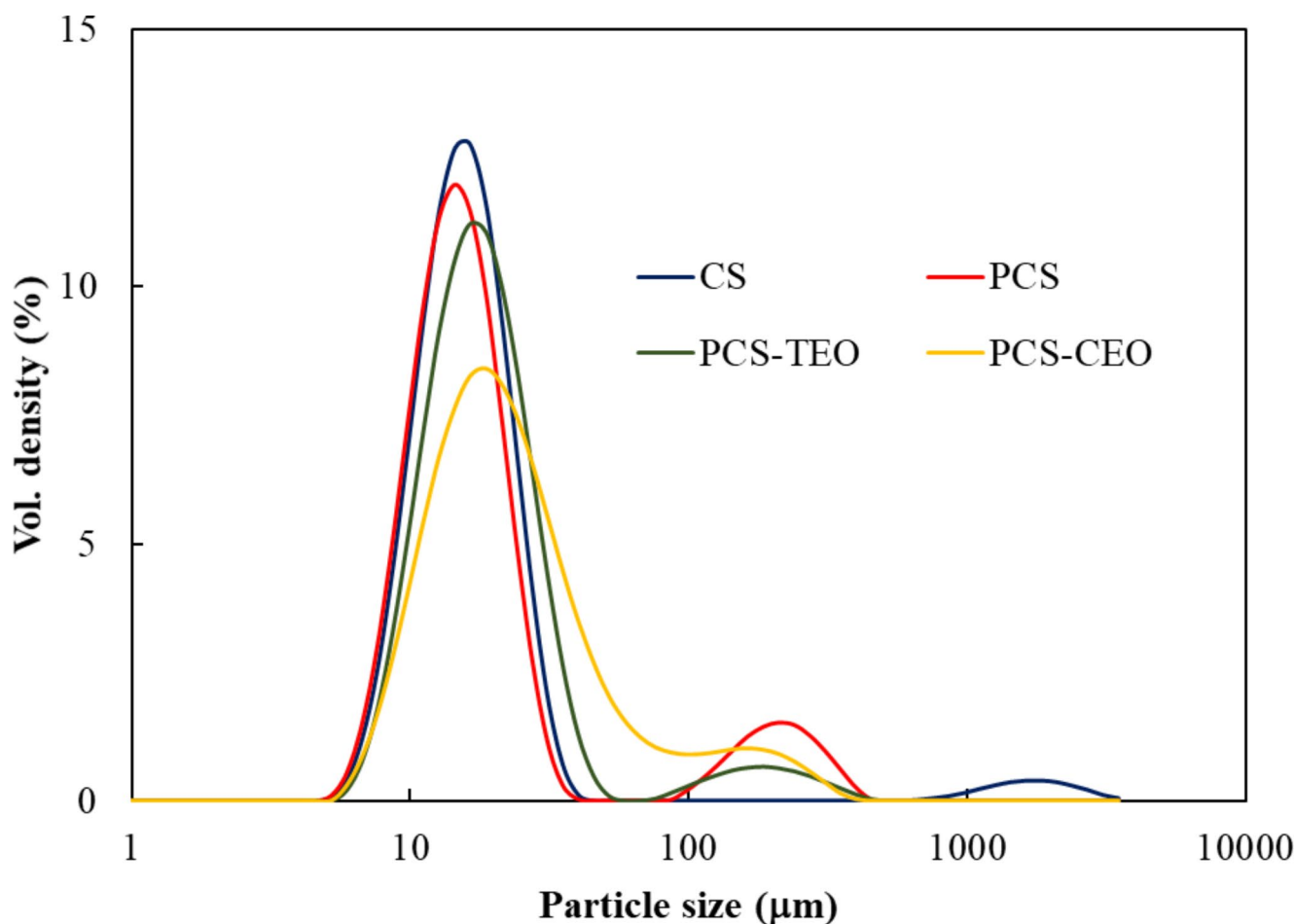


Fig. 1 Particle size distributions of native and porous corn starch, and EO encapsulated powders

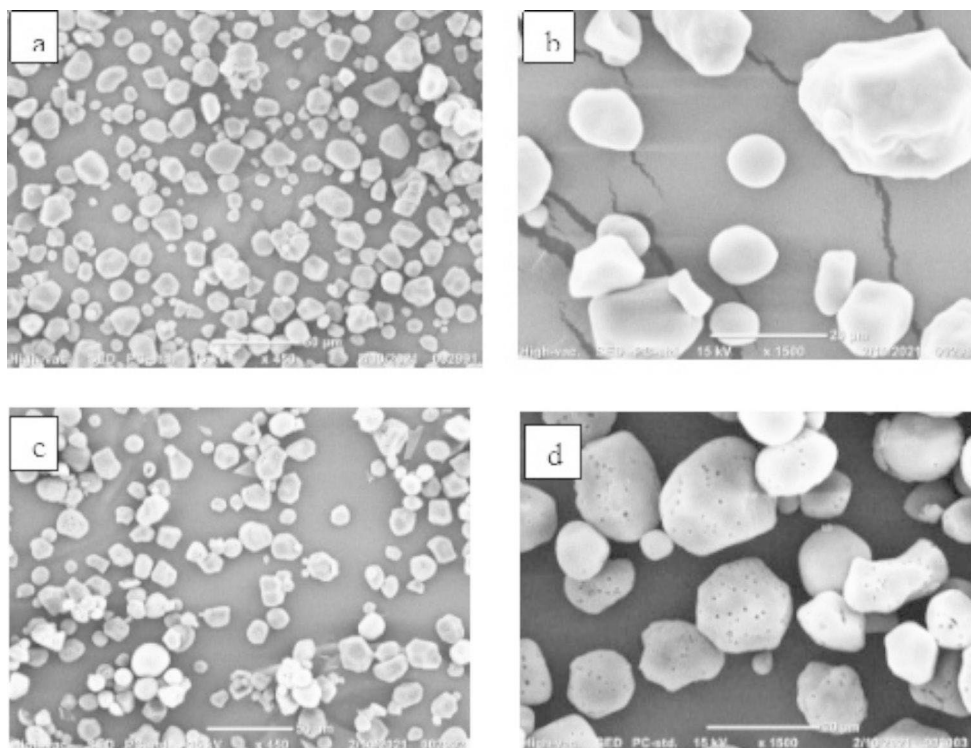
particle size because of the poor encapsulation efficiency (Table 2). Conversely, the enzyme-treated porous starch had a significant effect on the particle size. Furthermore, IC formed by EO in XG emulsion demonstrated that incorporation of XG had little effect on the size and diameter of the microcapsules. The PCS/TEO/XG encapsulates showed a bimodal distribution of particles with a reducing peak height and a slight shift to the right direction, indicating size enlargement. Following the PCS, the first peak was a range between 5 and 67- μm while particles with a size range between 67 and 454 were encompassed in the minor second peak. On the other hand, PCS/CEO/XG exhibited a unimodal distribution of particles with a hump and covered a range of particles between 5 and 400- μm . The peak height of the first peak for both microcapsules was superimposed at 18.7- μm . Upon inclusion complex formation, the particle size of the encapsulated starch increased for D_{v10} , D_{v50} when compared to the PCS. The D_{v10} values for PCS/TEO and PCS/CEO were 10.9 ± 0.89 - μm and 11.3 ± 0.79 - μm and the corresponding values were 18.8 ± 1.03 - μm and 22.5 ± 1.11 - μm for D_{v50} . Conversely, the D_{v90} values were

reduced for both encapsulated particles to 35.6 ± 1.58 - μm and 81.0 ± 2.33 - μm . These data indicate that the mean particle sizes of the inclusion complexes were significantly larger than the PCS; however, they significantly influenced the overall size (D_{v90}). Such a change has been influenced by many factors, including complex formation, drying, and size reduction. The sample span values varied between the two encapsulates. The encapsulate containing TEO has a superior distribution of particles over the CEO, as indicated by a lower S value of PCS/TEO (1.31 ± 0.47) against PCS/CEO (3.09 ± 0.79).

Surface morphology

Micrographs of native and porous corn starch at two selected magnifications (400 \times and 1500 \times) are shown in Fig. 2. The corn starch granules showed various shapes, starting from oval to round to polygonal or irregular shapes with smooth edges, and these observations are consistent with earlier reports [30, 31]. No pores or holes were present in the native starch. The enzymatic treatment of corn starch granules did

Fig. 2 Scanning electron micrographs of corn starch: (a) and (b) control at $\times 450$ and $\times 1500$, (c) and (d) porous at $\times 450$ and $\times 1500$



not influence the microstructure, and it was retained at the highest level (Fig. 2c) with multiple pore formation around the starch granules (Fig. 2d). A combination of enzymes [e.g., α -Amylase and amyloglucosidase (AMG)] has acted on the starch granules and created a significant number of pores on the surface of the starch granule. These observations are consistent with those reported earlier for corn starch [20, 32]. Dura et al. [20] further established that the pores generated by α -amylase were smaller in size (0.15- μm) when compared to AMG-treatment (1.72- μm), and therefore, it can be concluded that AMG has a stronger effect on the surface pore creation of starch. AMG created openings in channels of corn starch to provide access to the interior of the granule, and the surface pores enlarge through channels from the hilum region toward the outside [33]. The micro-encapsulation of EO/XG emulsion in PCS resulted in aggregates of particles and the distribution of EO into starch pores (Fig. 3a-d). A higher penetration of EO has been supported by higher encapsulation efficiency, as discussed earlier.

FTIR spectroscopy

The FTIR spectrum of the TEO exhibited three distinct absorption bands at 2959 cm^{-1} , 2925 cm^{-1} and 2870 cm^{-1} corresponding to the C-H stretching vibration of the methylene group (Fig. 4). The characteristic peaks exist in the range of 1200 to 1700 cm^{-1} , corresponding to the thymol phenolic groups of C=C stretching, C-O stretching, and

O-H bending [34]. On the other hand, the spectra of the CEO showed the absorption bands correspond to symmetric and antisymmetric -CH₂ and C-H bond stretching for alkane at 3075 , 3002 , and 2936 cm^{-1} . Furthermore, CEO aromatic compounds (phenols, aldehydes, and ketone) are represented by various bands at 1605 , 1511 and 1430 cm^{-1} that correspond to stretching vibrations of C=O, C=C, and -OH groups [35, 36].

The spectra of corn starch have broad absorption bands at 3315 cm^{-1} owing to O-H stretching vibration of starch resulting from inter or intramolecular interaction of the -OH bond [37]. Distinct bands at 2931 cm^{-1} and 1648 cm^{-1} , corresponding to the stretching vibration of C-H and the bending vibration of OH, were identified. The observed bands at 1150 , 1077 , and 990 are related to the stretching vibration of the C-O bond. The bands at 1077 and 990 cm^{-1} correspond to symmetric stretching of the C-O-C group [38]. Enzymatic treatment did not show any major shift in absorption bands, which infers that these treatments keep the chemical groups of starch intact. Similar observations were reported by Liu et al. [39] for corn starch.

The FTIR spectra of EO encapsulated in PCS demonstrated three major bands. The band detected at 3316 cm^{-1} corresponded to CS shifting to 3330 cm^{-1} in microcapsules. However, the band was widened and intense due to incorporation of the EO. Similarly, the band at 2931 cm^{-1} showed an increase in intensity for the CEO encapsulated microcapsules. Conversely, the TEO-based microcapsules showed the appearance of a new band at 2928 cm^{-1} , which

Fig. 3 Scanning electron micrographs of encapsulated corn starch: **(a)** and **(b)** PCS/CEO/XG at $\times 450$ and $\times 1500$, **(c)** and **(d)** PCS/TEO/XG at $\times 450$ and $\times 1500$

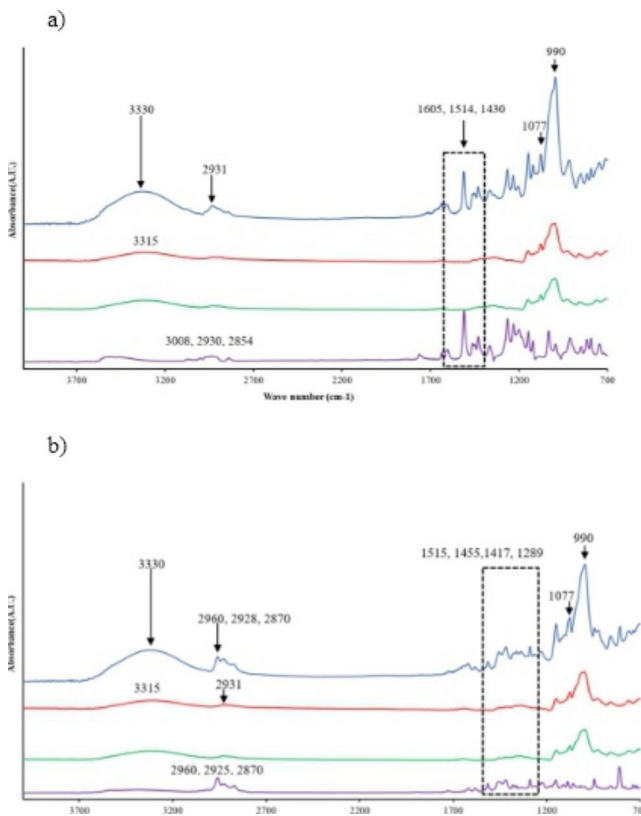
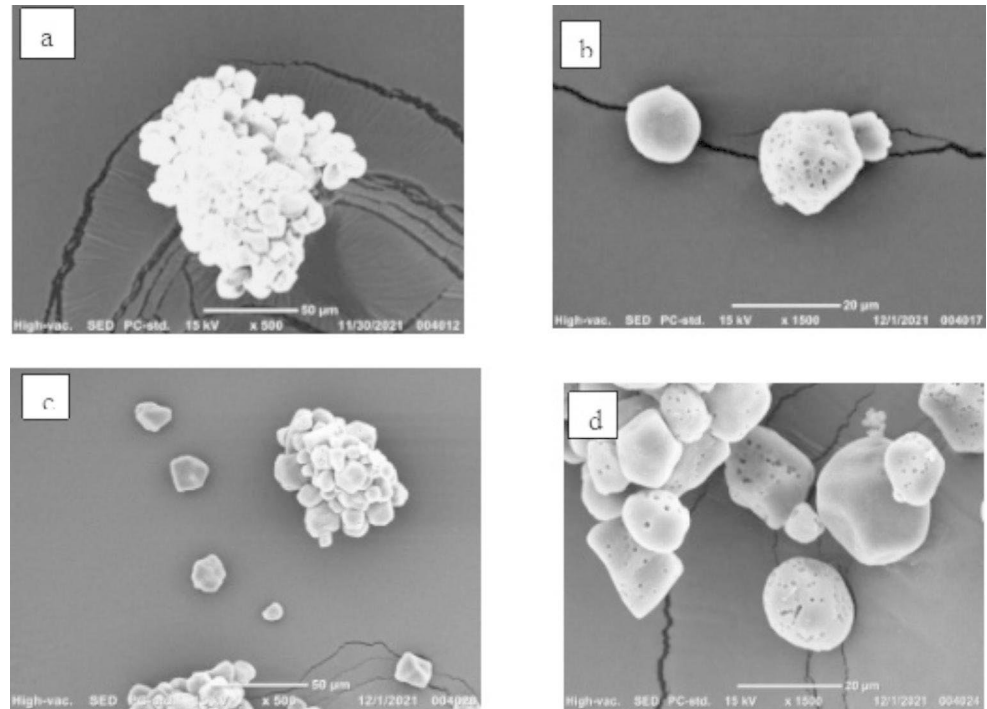


Fig. 4 FTIR spectra of porous corn starch and essential oil microcapsules **a)** Cinnamon essential oil **b)** Thyme essential oil (— Essential Oil; — Corn starch; — Gelatinized corn starch; — Enzyme treated corn starch; — Porous corn starch & essential oil microcapsule (pestle and mortar); — Porous corn starch & essential oil microcapsule (Gum)

could have occurred because of the merger of bands corresponding to TEO at 2920 cm^{-1} and CS at 2931 cm^{-1} . Similar results were observed for the porous potato starch/CEO nanocapsule [40]. These findings confirm the formation of EO/PCS microcapsules. However, no significant difference in spectra was observed with reference to the encapsulating methods.

Differential scanning calorimetry (DSC)

The thermal properties of the native, porous starches and their inclusion complexes were studied on a DSC to understand their interactions. The enzymatic treatment of native corn starch induced a shift in the endothermic peak from 106.03 to $121.81\text{ }^{\circ}\text{C}$ followed by porosity development in the starch granule (Fig. 5a). The corresponding fusion enthalpy (DH) of the PCS doubled (218.5 J/g) when compared with the native CS (102.3 J/g). It indicates the PCS is quite thermally stable over the CS. Both the CEO and TEO exhibited three thermograms. The peaks were detected at 140.65 , 171.81 , and $187.67\text{ }^{\circ}\text{C}$ for CEO, with the corresponding enthalpy values of 90.19 , 1.03 , and 12.10 J/g , respectively (Fig. 5b). Similarly, TEO had peaks at 115.03 , 152.66 , and $164.24\text{ }^{\circ}\text{C}$ with enthalpies of 29.14 , 3.81 , and 13.93 J/g , respectively (Fig. 5c). It indicates the CEO was thermally stable over the TEO. The TEO peak was not detected in the IC complex (PCS/TEO/XG) (Fig. 5c), suggesting the formation of molecular encapsulation of the oil inside the PCS cavity [16, 41]. The encapsulated first melting peak (T_m) at $108.63\text{ }^{\circ}\text{C}$ differs from the parent

Fig. 5 DSC thermograms of encapsulated corn starch: (a) comparison between native corn starch (CS) and porous corn starch (PCS) (b) influence of individual component to inclusion complex of PCS/TEO/XG.

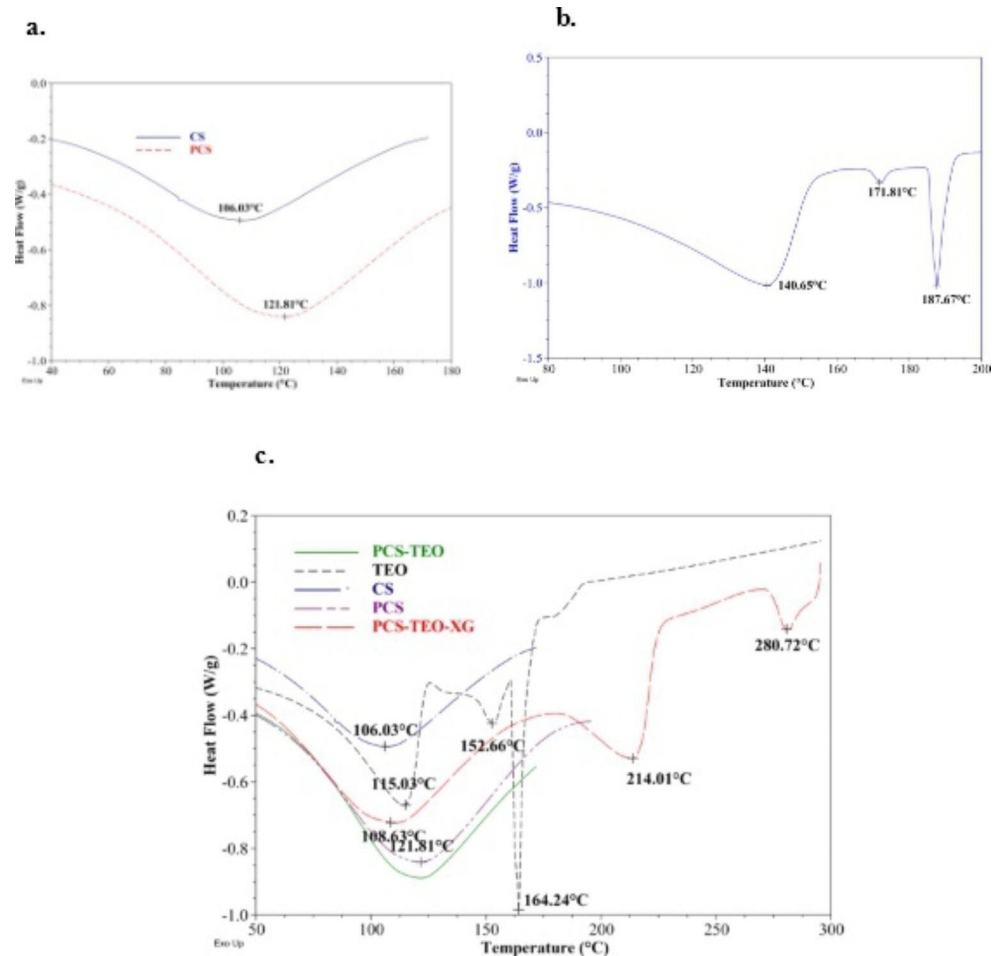


Table 3 Minimum inhibitory concentration (MIC) and minimum bactericidal concentration (MBC) for *Listeria monocytogenes* and *S. Typhimurium* for thyme and cinnamon essential oil and powdered inclusion complexes

Sample	<i>L. monocytogenes</i>		<i>S. Typhimurium</i>	
	MIC ($\mu\text{g/mL}$)	MBC ($\mu\text{g/mL}$)	MIC ($\mu\text{g/mL}$)	MBC ($\mu\text{g/mL}$)
CEO	2500 ^a	3000 ^a	2000 ^b	2500 ^b
TEO	1500 ^a	2000 ^a	1500 ^a	2000 ^a
PCS/CEO/XG	3500 ^a	4000 ^a	3000 ^b	3500 ^b
PCS/TEO/XG	2000 ^a	2500 ^a	2000 ^a	2500 ^a

†Values based on the actual concentrations of EO present on the inclusion complexes

All values are means \pm SD, n=3; values in the same row (MIC in one group and MBC in a separate group) with different letters are significantly different ($p < 0.05$)

PCS molecule. Furthermore, two distinct endotherms were detected at 214.01 (ΔH : 25 J/g) and 280.72 °C (ΔH : 6.5 J/g), and those peaks are believed to be attributed to the melting of corn starch. Oliyaei et al. [42] reported that the peak temperature for native and porous starch was 317 °C and there was no difference after the treatment. Zhong & Sun [43], on the other hand, discovered two T_m peaks at 182 and 195 °C with about 11% moisture content, which they attributed to the melting of cornstarch crystals and amylose-lipid complexes, respectively. Such variations have been attributed to the source of starch, preparation methods, and many other intrinsic factors. Overall, the encapsulated samples exhibit the formation of a good inclusion complex.

Antimicrobial activities of CD inclusion complexes

The antibacterial activity of free and loaded CEO and TEO in PCS was evaluated using *Listeria monocytogenes* (Gram-positive) and *S. Typhimurium* (Gram-negative) as test organisms. Table 3 presents the MIC and MBC results of the EO and ICs against *L. monocytogenes* and *S. Typhimurium*. The thyme essential oil (TEO) showed its excellent antimicrobial capabilities against *L. monocytogenes* and *S.*

Typhimurium with significantly lower values of MIC (1750 µg/mL) and MBC (2250 µg/mL) (Table 3), and these values were marginally lower than our earlier report [17]. On the other hand, *S. Typhimurium* had higher antimicrobial activity with lower MIC (2000 µg/mL) and MBC values (2500 µg/mL) than *L. monocytogenes* (MIC: 2500 µg/mL and MBC: 3000 µg/mL) against the CEO.

TEO encapsulates exhibited strong antibacterial activity against *L. monocytogenes* and *S. Typhimurium*, demonstrating broad-spectrum antibacterial activity against gram-positive and gram-negative bacteria. The minimum inhibitory concentration (MIC) and minimum bactericidal concentration (MBC) values of PCS/TEO/XG were 2000 µg/mL and 2500 µg/mL. While we compare the obtained microbial data with our earlier work on encapsulation of TEO in cyclodextrins (CDs) as wall materials (β - and γ -cyclodextrin) (MIC: 3500–4500 µg/mL and MBC: 4000–5000 µg/mL) [17] [1], it was found that PCS acts as a superior wall material than CDs. The active compounds present in thyme oil, including thymol, ρ -cymene and γ -terpinene have significantly contributed to imparting antimicrobial properties to the encapsulates [44]. Similar observations have been made on TEO when encapsulated in γ -cyclodextrin (GCD) wall matrix at a ratio (GCD:TEO) of 80/20 (w/w) [1]. On the other hand, CEO showed higher antimicrobial activity against *S. Typhimurium* (MIC: 3000 µg/mL and MBC: 3500 µg/mL) when compared to *L. monocytogenes* (MIC: 3500 µg/mL and MBC 4000 µg/mL). The obtained results revealed that the CEO is more effective against gram-negative bacteria and this observation is consistent with an earlier study using GCD as a wall material [16]. However, it was found that PCS acts as a better wall material when compared to cyclodextrins [16]. Previously, a lower MIC and MBC of 2500 ppm were reported for the CEO against *E. coli* [45]. The higher MIC and MBC values obtained in this study could be attributed to the lack of a solvent in the encapsulation process, which was previously used to increase the dispersion of the essential oil in water. Overall, it can be concluded that TEO acts as a superior antimicrobial agent than CEO against both gram-positive and gram-negative organisms in the formation of porous starch-based encapsulates.

Conclusions

The excess inexpensive starch can be converted to porous corn starch so that it can be used as a wall material during the encapsulation of bioactive compounds. Selective enzymatic treatments produce pores in the corn starch surface, improving hydration and oil-holding capacity. Particles remained constant during the conversion of native starch to porous starch. However, they increased significantly

with agglomeration after essential oil was entrapped in the PCS matrix. A moderate encapsulation efficiency has been observed when emulsified essential oil and xanthan gum solution are entrapped in a porous starch matrix, which has been further confirmed using the FTIR, DSC, and SEM. Thyme essential oil entrapped in PCS exhibits excellent antimicrobial activity against both gram-positive and gram-negative pathogens. The developed encapsulated powders have potential applications in food and pharmaceutical products or in the development of active packaging by controlling the release of EO.

Acknowledgements The author expresses their gratitude to Kuwait Foundation for Advancement of Science (KFAS; Grant number: PR18-13MM-02) and Kuwait Institute for Scientific Research for providing the grant for the research work (Grant number FB133C).

Authors Contribution Jasim Ahmed: conceptualization, methodology, Resources, writing - review & editing, Supervision, Project administration. L. Thomas: Sample preparation and formal analysis; M. Mulla: FTIR; S. Al-Jassar: SEM analysis; Harsha Jacob: microbiological analysis. All authors read and approved the final manuscript.

Declarations

Competing interests The authors do not have any conflict of interest.

References

1. J. Ahmed, M.Z. Mulla, H. Al-Attar, H. Jacob, (2022). Comparison of thermo-rheological, microstructural and antimicrobial properties of β - and γ -cyclodextrin inclusion complexes of cinnamon essential oil. *J. Food Measur. Char.* 16, 3010–3022 (2022). <https://doi.org/10.1007/s11694-022-01404-3>
2. S.A. Burt, R. Vlieland, H.P. Haagsman, E.J. Veldhuizen, Increase in activity of essential oil components carvacrol and thymol against *Escherichia coli* O157:H7 by addition of food stabilizers. *J. Food Prot.* 68(5), 919–926 (2005). <https://doi.org/10.4315/0362-028x-68.5.919>
3. M. Azizi-Lalabadi, Z. Rahimzadeh-Sani, J. Feng, H. Hosseini, S.M. Jafari, The impact of essential oils on the qualitative properties, release profile, and stimuli-responsiveness of active food packaging nanocomposites. *Crit. Rev. Food Sci. Nutr.* 63(13), 1822–1845 (2023). <https://doi.org/10.1080/10408398.2021.1971154>
4. W. Weisany, J. Amini, S. Samadi, S. Hossaini, S. Yousefi, P.C. Struik, Nano silver-encapsulation of *Thymus daenensis* and *Anethum graveolens* essential oils enhances antifungal potential against strawberry anthracnose. *Ind. Crops Prod.* 141, 111808 (2019). <https://doi.org/10.1016/j.indcrop.2019.111808>
5. J. Ahmed, Y.A. Arfat, A. Bher, M. Mulla, H. Jacob, R. Auras, Active chicken meat packaging based on polylactide films and bimetallic Ag-Cu nanoparticles and essential oil. *J. Food Sci.* 83, 1299–1310 (2018). <https://doi.org/10.1111/1750-3841.14121>
6. M. Cisarová, J. Kačínová, D. Tančínová, Antifungal activity of selected essential oils against the fungal species the genus *eurotium* by contact vapour. *J. Microbiol. Biotechnol. Food Sci.* 9(4), 202–205 (2020)

7. M.M. Moshaverinia, A. Rastegarfar, F. Moattari, F. Lavaee, Evaluation of the effect of hydro alcoholic extract of cinnamon on herpes simplex virus-1. *Dent. Res J.* **17**(2), 114 (2020)
8. F. Hu, X.-F. Tu, K. Thakur, F. Hu, X.-L. Li, Y.-S. Zhang et al., Comparison of antifungal activity of essential oils from different plants against three fungi. *Food Chem. Toxicol.* **134**, 110821 (2019). <https://doi.org/10.1016/j.fct.2019.110821>
9. K. Yang, A. Liu, A. Hu, J. Li, Z. Zen, Y. Liu, S. Tang, C. Li, Preparation and characterization of cinnamon essential oil nanocapsules and comparison of volatile components and antibacterial ability of cinnamon essential oil before and after encapsulation. *Food Control.* **123**, 107783 (2021). <https://doi.org/10.1016/j.foodcont.2020.107783>
10. M. Ghasemi, M.A. Miri, M.A. Najafi, M. Tavakoli, T. Hadadi, Encapsulation of cumin essential oil in zein electrospun fibers: characterization and antibacterial effect. *J. Food Measur Char.* **16**, 1613–1624 (2022). <https://doi.org/10.1007/s11694-021-01268-z>
11. S.C. Purcell, P. Pande, Y. Lin, E.J. Riveria et al., Extraction and antibacterial properties of thyme leaf extracts: authentic practice of green chemistry. *J. Chem. Edu.* **93**, 1422–1427 (2016). <https://doi.org/10.1021/acs.jchemed.5b00891>
12. X. Wang, H.D. Goff, S.W. Cui, Comparison of synergistic interactions of yellow mustard gum with locust bean gum or κ -carrageenan. *Food Hydrocoll.* **132**, 107804 (2022). <https://doi.org/10.1016/j.foodhyd.2022.107804>
13. A.P.R. Charles, T.Z. Jin, R. Mu, Y. Wu, Electrohydrodynamic processing of natural polymers for active food packaging: a comprehensive review. *Compr. Rev. Food Sci. Food Saf.* **20**(6), 6027–60561 (2021). <https://doi.org/10.1111/1541-4337.12827>
14. H. Bao, H.H. Ding, A.P.R. Charles, D. Hui, S. Rakshit, S. Nahashon, Y. Wu, Application of yellow mustard mucilage in encapsulation of essential oils and polyphenols using spray drying. *Food Hydrocoll.* **143**, 108815 (2023). <https://doi.org/10.1016/j.foodhyd.2023.108815>
15. S.K. Sundar, J.K. Parikh, Advances and trends in encapsulation of essential oils. *Int. J. Pharmaceu.* **635**, 122668 (2023). <https://doi.org/10.1016/j.ijpharm.2023.122668>
16. J. Ahmed, M.Z. Mulla, H. Al-Attar et al., Thermal, structural, antimicrobial and physicochemical characterization of thyme essential oil encapsulated in β - and γ -cyclodextrin. *J. Microencap.* **39**(4), 364–379 (2022b). <https://doi.org/10.1080/02652048.2022.2090626>
17. W. Weisany, S. Yousefi, N.A. Tahir, N. Golestanezhadeh, D.J. McClements, B. Adhikari et al., Targeted delivery and controlled release of essential oils using nanoencapsulation: a review. *Adv. Colloid Interface Sci.* **303**, 102655 (2022). <https://doi.org/10.1016/j.cis.2022.102655>
18. H.A. Romero-Hernandez, M.M. Sánchez-Rivera, J. Alvarez-Ramirez, H. Yee-Madeira, J. Yañez-Fernandez, L.A. Bello-Pérez, Avocado oil encapsulation with OSA-esterified taro starch as wall material: Physicochemical and morphology characteristics. *LWT.* **138**, 110629 (2021). <https://doi.org/10.1016/j.lwt.2020.110629>
19. B. Zhang, D. Cui, M. Liu, H. Gong, Y. Huang, F. Han, Corn porous starch: preparation, characterization and adsorption property. *Int. J. Biol. Macromol.* **50**, 250–256 (2012). <https://doi.org/10.1016/j.ijbiomac.2011.11.002>
20. A. Dura, W. Błaszczak, C.M. Rosell, Functionality of porous starch obtained by amylase or amyloglucosidase treatments. *Carbohydr. Polym.* **101**, 837–845 (2014). <https://doi.org/10.1016/j.carbpol.2013.10.013>
21. L. Wu, J. Tian, X. Ye, H. Fang, Z. Zhang, C. Xu, H. Zhang, Encapsulation and Release of Curcumin with the mixture of Porous Rice Starch and Xanthan Gum. *Starch/ Stärke.* **73**, 2000042 (2020). <https://doi.org/10.1002/star.202000042>
22. J. Ahmed, J., Effect of particle size and temperature on rheology and creep behavior of barley β -d-glucan concentrate dough. *Carbohydr. Polym.* **111**, 89–100 (2014). <https://doi.org/10.1016/j.carbpol.2014.03.098>
23. H. Huang, C. Huang, C. Yin, M.R.U. Khan, H. Zhao, Y. Xu, L. Huang, L.D. Zheng, M. Qi, Preparation and characterization of β -cyclodextrin–oregano essential oil microcapsule and its effect on storage behavior of purple yam. *J. Sci. Food Agri.* **100**, 4849–4857 (2020). <https://doi.org/10.1002/jsfa.10545>
24. Y. Xie, B. Zhang, M.-N. Li, H.-Q. Chen, Effects of cross-linking with sodium trimetaphosphate on structural and adsorptive properties of porous wheat starches. *Food Chem.* **289**, 187–194 (2019). <https://doi.org/10.1016/j.foodchem.2019.03.023>
25. L. Guo, R. Liu, X. Li, Y. Sun, X. Du, The physical and adsorption properties of different modified corn starches. *Starch/Stärke.* **67**, 237–246 (2015). <https://doi.org/10.1002/star.201400200>
26. G. Chen, B. Zhang, Hydrolysis of granular corn starch with controlled pore size. *J. Cereal Sci.* **56**, 316–320 (2012). <https://doi.org/10.1016/j.jcs.2012.01.011>
27. J.D. Hoyos-Leyva, L.A. Bello-Pérez, J. Alvarez-Ramirez, H.S. Garcia, Microencapsulation using starch as wall material: a review. *Food Rev. Int.* **34**(2), 148–161 (2018). <https://doi.org/10.1080/87559129.2016.1261298>
28. X. Cai, X. Du, D. Cui, X. Wang, Z. Yang, G. Zhu, Improvement of stability of blueberry anthocyanins by carboxymethyl starch/xanthan gum combinations microencapsulation. *Food Hydrocoll.* **91**, 238–245 (2019). <https://doi.org/10.1016/j.foodhyd.2019.01.034>
29. M. Marek Molenda, M. Stasiak, J. Horabik, J. Fornal, W. Błaszczak, A. Ornowski, Microstructure and mechanical parameters of five types of starch. *Pol. J. Food Nutr. Sci.* **15/56**, 161–168 (2006)
30. C. Pukkahuta, B. Suwannawat, S. Shobsngob, S. Varavinit, Comparative study of pasting and thermal transition characteristics of osmotic pressure and heat–moisture treated corn starch. *Carbohydr. Polym.* **72**(3), 527–536 (2008). <https://doi.org/10.1016/j.carbpol.2007.09.024>
31. D. Xie, X. Liu, H. Zhang, W. Xia, X. Huang, D. Bi, S. Pan, Textural properties and morphology of soy 7S globulin-corn starch (amylose, amylopectin). *Int. J. Food Proper.* **20**(10), 2197–2205 (2017). <https://doi.org/10.1080/10942912.2016.1233430>
32. A.-Q. Zhao, L. Yu, M. Yang, C.-J. Wang, M.-M. Wang, X. Bai, Effects of the combination of freeze-thawing and enzymatic hydrolysis on the microstructure and physicochemical properties of porous corn starch. *Food Hydrocoll.* **83**, 465–472 (2018). <https://doi.org/10.1016/j.foodhyd.2018.04.041>
33. K.C. Huber, J.N. BeMiller, Channels of maize and sorghum starch granules. *Carbohydr. Polym.* **41**, 269–276 (2000). [https://doi.org/10.1016/S0144-8617\(99\)00145-9](https://doi.org/10.1016/S0144-8617(99)00145-9)
34. A. Celebioglu, Z.I. Yildiz, T. Uyar, Thymol/cyclodextrin inclusion complex nanofibrous webs: enhanced water solubility, high thermal stability and antioxidant property of thymol. *Food Res. Int.* **106**, 280–290 (2018). <https://doi.org/10.1016/j.foodres.2017.12.062>
35. R. Bagheri, P. Ariaii, A. Motamedzadegan, Characterization, antioxidant and antibacterial activities of chitosan nanoparticles loaded with nettle essential oil. *J. Food Measur Char.* **15**, 1395–1402 (2021). <https://doi.org/10.1007/s11694-020-00738-0>
36. Y. Wang, C. Yuan, Y. Liu, B. Cui, Fabrication of kappa-carrageenan hydrogels with cinnamon essential oil/ hydroxypropyl- β -cyclodextrin composite: evaluation of physicochemical properties, release kinetics and antimicrobial activity. *Int. J. Biol. Macromol.* **170**, 593–601 (2021). <https://doi.org/10.1016/j.ijbiomac.2020.12.176>
37. P.C. Flores-Silva1, C.A. 1 Roldan-Cruz, G. Chavez-Esquivel, E.J. Vernon-Carter, L.A. Bello-Perez, Alvarez-Ramirez, In vitro digestibility of ultrasound-treated corn starch. *Starch/Stärke.* **69**, 1700040 (2017). <https://doi.org/10.1002/star.201700040>

38. K. Ponsanti, B. Tangnorawich, N. Ngernyuang, Pechyen, flower shape-green synthesis and characterization of silver nanoparticles (AgNPs) with different starch as a reducing agent. *J. Mater. Res. Technol.* **9**(5), 11003–11012 (2020). <https://doi.org/10.1016/j.jmrt.2020.07.077>
39. Z. Liu, C. Wang, X. Liao, Q. Shen, Measurement and comparison of multi-scale structure in heat and pressure treated corn starch granule under the same degree of gelatinization. *Food Hydrocoll.* **108**, 106081 (2020). <https://doi.org/10.1016/j.foodhyd.2020.106081>
40. Y. Fang, J. Fu, P. Liu, B. Cu, Morphology and characteristics of 3D nanonetwork porous starch-based nanomaterial via a simple sacrifice template approach for clove essential oil encapsulation. *Ind. Crops Prod.* **143**, 111939 (2020). <https://doi.org/10.1016/j.indcrop.2019.111939>
41. C. Gomes, R.G. Moreira, E. Castell-Perez, Microencapsulated antimicrobial compounds as a means to enhance electron beam irradiation treatment for inactivation of pathogens on fresh spinach leaves. *J. Food Sci.* **76**, E479–E488 (2011). <https://doi.org/10.1111/j.1750-3841.2011.02264.x>
42. N. Oliyaei, M. Moosavi-Nasab, A.M. Tamaddon, M. Fazaeli, Preparation and characterization of porous starch reinforced with halloysite nanotube by solvent exchange method. *Int. J. Biol. Macromol.* **123**, 682–690 (2019). <https://doi.org/10.1016/j.ijbiomac.2018.11.095>
43. Z. Zhong, S. Sun, Thermal characterization and phase behavior of cornstarch studied by differential scanning calorimetry. *J. Food Eng.* **69**(4), 453–459 (2005). <https://doi.org/10.1016/j.jfoodeng.2004.07.023>
44. M. Ben Jabeur, L. Somai-Jemmali, W. Hamada, Thyme essential oil as an alternative mechanism: biofungicide-causing sensitivity of *Mycosphaerella graminicola*. *J. App Microbiol.* **122**, 932–939 (2017). <https://doi.org/10.1111/jam.13408>
45. M. Raeisi, H. Tajik, J. Aliakbarlu, S. Hamed, M.H.S. Hosseinie, Effect of carboxymethyl cellulose-based coatings incorporated with *Zataria multiflora* Boiss. Essential oil and grape seed extract on the shelf life of rainbow trout fillets. *Lwt. Food Sci. & Technol.* **64**, 898–899 (2015). <https://doi.org/10.1016/j.lwt.2015.06.010>

Publisher's Note Springer Nature remains neutral with regard to jurisdictional claims in published maps and institutional affiliations.

Springer Nature or its licensor (e.g. a society or other partner) holds exclusive rights to this article under a publishing agreement with the author(s) or other rightsholder(s); author self-archiving of the accepted manuscript version of this article is solely governed by the terms of such publishing agreement and applicable law.